Theor Chem Account (2008) 121:91–101
DOI 10.1007/s00214-008-0453-4

REGULAR ARTICLE

Thermal [1,3] sigmatropic rearrangements of bicyclic and tricyclic vinylcyclobutanes: a gray zone between the concerted and stepwise extremes

Hai-Rong Tao · De-Cai Fang

Received: 9 February 2008 / Accepted: 24 April 2008 / Published online: 14 May 2008

Abstract Four typical thermal [1,3] sigmatropic rearrangements of bicyclic and tricyclic vinylcyclobutanes and one fancied analogous reaction (R2 in Scheme 1) were examined using CASSCF, CASPT2 and CAS+1+2 methods to discern the reaction mechanisms. Computed results indicate that it is difficult to simply designate these reactions as traditional single-step concerted or stepwise mechanisms, but a situation locating between these two extremes seems to be reasonable. The extent the reaction exhibits as a single-step concerted or stepwise path is much dependent on the geometrical constraints of reactant. For example, the system with three-member ring will tend to behave like a single-step concerted process, where only one rotation movement around C–C bond could be found when the bridged C–C is broken. However, the species with four-member ring will be much closer to the stepwise mechanism involving diradical varieties, because there are two different rotation movements exist when the bridged C–C is broken. Our calculation will also rationalize that only suprafacial retention product could be yielded for the thermal [1,3] sigmatropic rearrangement of tricyclic vinylcyclobutane.

Keywords Sigmatropic rearrangement · Vinylcyclobutanes · Reaction mechanism · CASSCF calculation · Suprafacial retention · Suprafacial inversion

Electronic supplementary material The online version of this article (doi:10.1007/s00214-008-0453-4) contains supplementary material, which is available to authorized users.

H.-R. Tao · D.-C. Fang (✉)
College of Chemistry, Beijing Normal University,
100875 Beijing, China
e-mail: dcfang@bnu.edu.cn

1 Introduction

The study of the gas-phase thermal [1,3] sigmatropic rearrangement has been over 40 years since Woodward and Hoffmann's selection rules for sigmatropic rearrangement reactions [1–4] and Berson's seminal work on the bicycle[3.2.0] hept-2-ene system [5–7]. Despite the fact that Frey had already formulated a mechanistically attractive analysis of the vinylcyclobutane to cyclohexene isomerization as a stepwise, diradical-mediated process [8,9], Woodward and Hoffmann's paradigm, when applied to [1,3] carbon sigmatropic rearrangement [1–4], proved appealing to many researchers. The controversy between the concerted mechanism that obeyed Woodward–Hoffmann selection rules and the stepwise pathway involving a diradical intermediate has continued into the present century.

The [1,3] carbon shift of 5-*exo*-methylbicyclo[2.1.1]hex-2-ene (**1A**) to 6-*exo*-methylbicyclo [3.1.0]hex-2-ene (**1B**) (**R1** in Scheme 1) [10] has been a convincing exemplar of Woodward–Hoffman selection rules, in which the ratio of symmetry-allowed suprafacial inversion (SI) product **1B** and symmetry-forbidden suprafacial retention (SR) product **1C** is 200:1 at the temperature of 120 °C. The [1,3] sigmatropic migration products of the substituted bicyclo[3.2.0]hept-2-enes were formed with more inversion than retention [5–7,11,12], but the measured ratio of SI/SR was dependent on the nature and stereochemical disposition of substituents and in some cases the temperature. A recent investigation [13] of 7-*exo*-methylbicyclo[3.2.0]hept-2-ene revealed that the isomerization reaction was with an SI/SR ratio of 6.8 (**R3** in Scheme 1). Bogle et al. [14] have recently confirmed that 8-*exo*-methylbicyclo[4.2.0]oct-2-ene (**R4** in Scheme 1) gives isomeric [1,3] carbon shift products a SI/SR ratio of 2.4, which is very similar to Berson and Holder's result (SI/SR = 2.2) that was reported for the isomerization reaction of

Scheme 1 [1,3] Sigmatropic rearrangements (**R1**–**R5**)

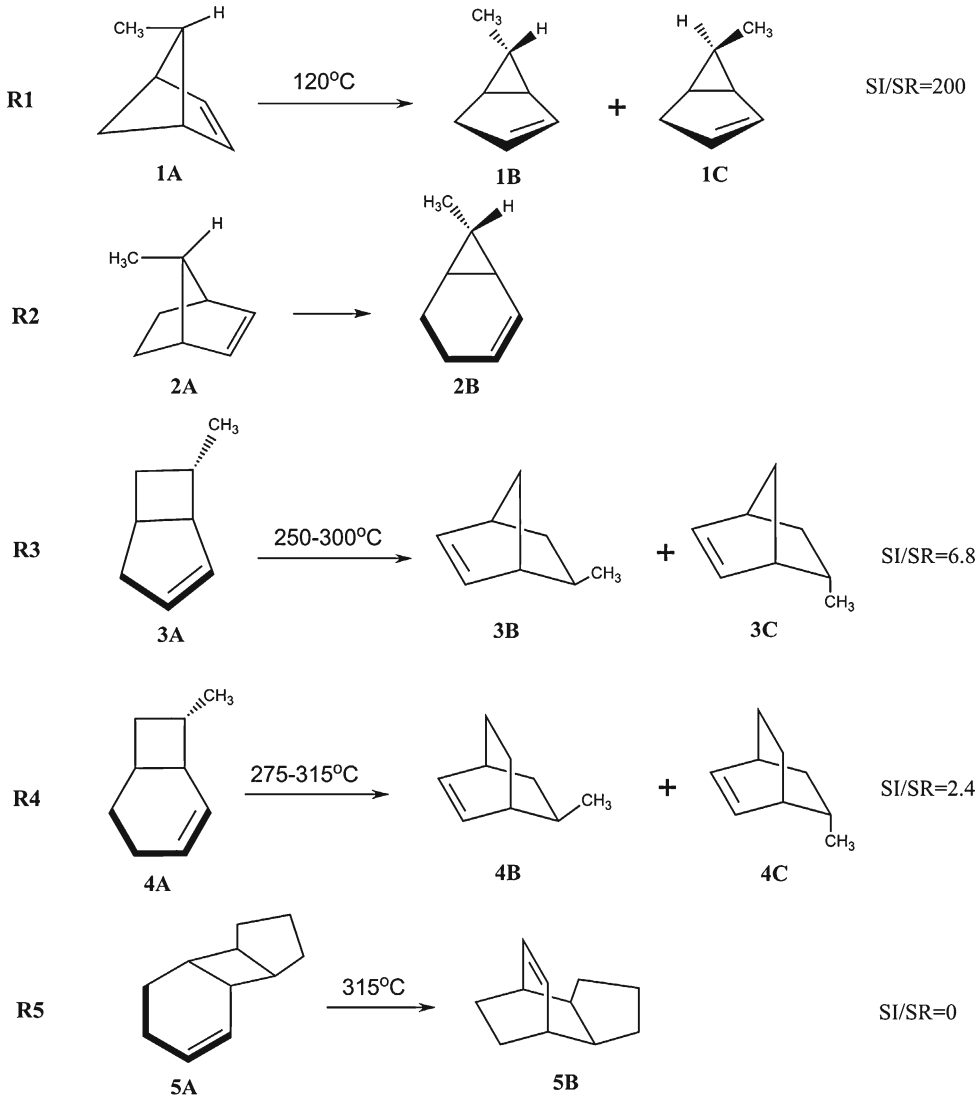

7-*endo*-acetoxy-8-*exo*-methylbicyclo[4.2.0]oct-2-ene [15]. In 2005, Baldwin et al. [16] found the first example of only SR product that was the thermal isomerization of *cis*,anti,*cis*-tricyclo [6.3.0.0^{2,7}]undec-3-ene to endo-tricyclo[5.2.2.0^{2,6}] undec-8-ene (**R5** in Scheme 1), and they derived that the geometrical constraints forced a symmetry-forbidden suprafacial retention outcome (SR product). In this paper, the reactions in Scheme 1 will be investigated with complete active space multiple reference self-consistent field (CASSCF), second-order perturbation (CASPT2) and multi-reference configuration interaction (MR-CI), in order to explore the relationships between geometric structures and reaction mechanisms.

2 Computational methods

The geometric parameters for all the possible stationary points involved in the reactions have been optimized by using a complete active space self-consistent field (CASSCF) calculation employing CAS(4,4)/6-31G(d,p) method, in which the active space includes two π electrons and two σ electrons and their relevant orbitals (π, π^*, σ, σ^*) that are related to the bond breaking and making. The geometric locations have been performed with GAUSSIAN-03 [17], MOLPRO,[1] and GAMESS [18] suite of programs, respectively, with which all of the structures have been converged to the same results. These structures thus obtained have also been confirmed with the vibrational frequencies and their number of the imaginary frequencies, in which all optimized transition states have been further elucidated by tracing intrinsic reaction

[1] MOLPRO is a package of ab initio programs written by Werner H-J, and Knowles PJ, with contributions from Almlof J, Amos RD, Berning A, Cooper DL, Deegan MJO, Dobbyn AJ, Eckert F, Elbert ST, Hampel C, Lindh R, Lloyd AW, Meyer W, Nicklass A, Peterson K, Pitzer R, Stone AJ, Taylor PR, Mura ME, Pulay P, Schutz M, Stoll H, Thorsteinsson T.

Scheme 2 [1, 3] Sigmatropic rearrangement of **1A** and **2A**, respectively (all distances are in Å and all angles are in degree)

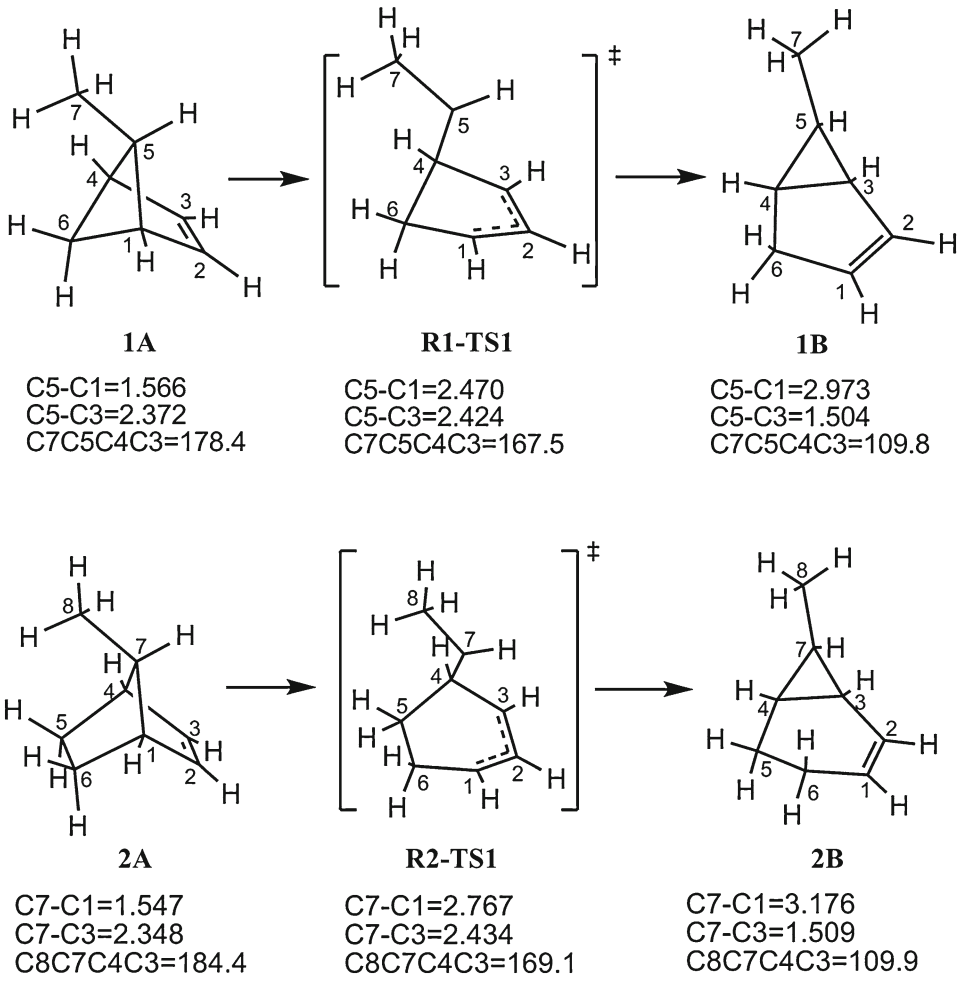

coordinate (IRC) [19–24] or dynamic reaction coordinate (DRC) [25–29] that were implemented in GAMESS suite of program [18]. The scaling factor 0.91 for frequencies and hence zero-point energies (ZPEs) has been obtained by comparing the computed frequencies with experimental results for species **3B** and **3C** [30]. In order to consider more accurate electron-correlation, the single-point multi-reference configuration interaction (MR-CI) calculations, including all single and double excitations relative to the CAS (4,4) reference wavefunctions, have been performed with MOLPRO suite of program. Such method was also denoted as CAS+1+2 [31,32]. In view of Borden's original work on the cope rearrangements [33,34], the internally contracted multi-reference second-order perturbation (CASPT2) [35] method is in excellent agreement with experimental results. Therefore, both CASPT2 and MR-CI [31,32] single-point calculations have been employed for comparison. To validate the calculated results, the G2 energies of all reactants and products involved in the reactions have also been calculated with GAUSSIAN-03 [17] to offset the absence of experimental data. Because the ZPEs have been included in G2 calculations, the scaled zero-point energies, obtained from CASSCF methods, have been added into the CASPT2 and MR-CI energies in order to compare those data with computed G2 energies.

3 Results and discussions

R1 and **R2.** The [1,3] carbon shift of 5-*exo*-methylbicyclo[2.1.1]hex-2-ene (**1A**) to 6-*exo*-methylbicyclo[3.1.0]hex-2-ene (**1B**), as illustrated in Scheme 2, has been an almost universally acceptable example that obeys Woodward–Hoffmann rule. The computed results indicate that the [1,3] carbon migration of **1A** indeed takes place asynchronously, but with only one transition state **R1-TS1**. In this transition state, the distance of C5–C1 is almost the same as that of C5–C3, indicating that the transition state is on the half way of the reaction path. It is reasonable that methyl group turns outward in replacement of inward to reduce the repulsion

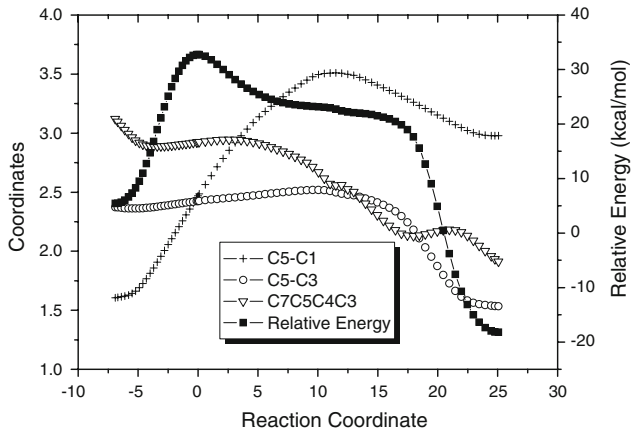

Fig. 1 Potential energy profile (kcal/mol) for the conversion of **1A** to **1B** and main geometric parameters of stationary points along the reaction pathway (here bond length in Å and dihedral angle in radian)

between methyl group and the ring, as observed in the change of the dihedral angle of C7C5C4C3 that is ranging from 178.4° in **1A** to 167.5° in **R1-TS1** and finally to 109.8° in **1B**. This movement behaves as the inversion of C5, and hence results in **1B**, a so-called symmetry-allowed SI product (see Scheme 2). The changes of the main geometric parameters and energies along the reaction path is depicted in Fig. 1, from which one can reveal that the key evolvement of the geometric parameters is on the distance of C5–C1 before **R1-TS1**, which contributes to the energy barrier for the reaction. The potential energy profile is very flat between $s = 2$ and $s = 18$ $(\text{amu})^{1/2}$bohr, as the distance changes of C5–C1 and C5–C3 are within the long range interaction, and have little influence on the total energy of the system, and the same as the torsion movement of the dihedral angle of C7C5C4C3 within this range. This finding is the same as Houk's statement [36] that there is no deep minimum on the potential energy surface and there is a large region where geometrical variations result in very small changes in energy. After $s = 18$ $(\text{amu})^{1/2}$bohr, the P orbital of C5 turns to the right orientation, favoring the overlap with one of P lobe of C3 in C=C π bonding, and thus lowering the total energy of the system due to the gradual formation of C5–C3 bonding, as illustrated in Fig. 2.

However, anatomizing the flat part of Fig. 1 indicates that some of the structures in this region are indeed of typical diradical, as observed in the Fig. 3, in which the populations of the active orbitals 2 and 3 tend to near one for structures of $s = 5$–15 $(\text{amu})^{1/2}$bohr. In these structures, one electron in one active orbital is mainly on C1–C2–C3 and another one is mainly on C5. The vibrational analysis along $s = 0$–15 $(\text{amu})^{1/2}$bohr showed that some interesting results have been observed. For $s = 0$–2.1 $(\text{amu})^{1/2}$bohr, each geometry has one imaginary frequency, the vibrational mode of which is closely related to the stretching movement of C1–C5, while for $s = 2.2$–2.8 $(\text{amu})^{1/2}$bohr, the imaginary frequency is disappeared. After $s = 2.8$ $(\text{amu})^{1/2}$bohr, this imaginary frequency occurs again, but the vibrational mode becomes the movement of rotation along C4–C5 bond. Suppose these two movements can be separated, i.e., the C1–C5 bond is broken completely before the rotation along C4–C5 bond, one can fix the torsional angle C7C5C4C3 from 160° to 220° and optimize other parameters, and then the potential energy profile, shown in Fig. 4, could be sketched. From Fig. 4, one can observe that there are one intermediate **R1-rINT**($\mathbf{R}_{C1-C5} = 3.64$ Å) and two transition states **R1-rTS1**($\mathbf{R}_{C1-C5} = 3.42$ Å) and **R1-rTS2**($\mathbf{R}_{C1-C5} = 3.60$ Å), respectively, in which **R1-rTS1** with smaller C7C5C4C3 angle is toward to SI product and **R1-rTS2** is connected to SR product. Obviously, **R1-rTS2** is with higher barrier because of larger repulsion between CH_3 and five-membered ring. This is in good agreement with the experimental ratio of SI/SR of 200:1. We have tried our best to locate the transition state between **1A** and **R1-rINT**, but it always failed. The geometry of **R1-rINT** is very close to that of the some point in the flat region of Fig. 1, so one cannot rule out the possibility of the formation of **R1-rINT** though it should be low.

The investigations from Carpenter group [37,38] for the [1,3] sigmatropic rearrangement of phenyl-substituted-bicyclo[2.1.1]hex-2-ene revealed that the experimental stereochemistry ratio results could be rationalized by the dynamic-controlling explanation, in which there involve the diradical intermediates along the reaction pathways. One can presume that the phenyl-substituents might enhance the stability of these intermediates and then drive the reaction to the diradical pathway.

The obtained potential energy profile for the conversion of **1A** to **1B** is also depicted in Fig. 5 (1), from which one can observe that the energy barrier for this conversion process is about 30(CAS + 0.91ZPE) or 32.1(MR-CI + 0.91ZPE) kcal/mol, which is in good agreement with the experimental condition that the reaction could proceed in 120°C. Comparing relative energies of **1B** from CASSCF, CASPT2 and MR-CI calculations with G2 energy, respectively, one can find that CASPT2 energy (−19.4 kcal/mol) is the closest to G2 energy (−18.4 kcal/mol).

Leigh [39] once investigated the [1,3]sigmatropic rearrangement of **2B** under direct photolysis and believed that the formation of the symmetry-allowed 7-*endo*-methylbicyclo[2.2.1]hept-2-ene proceeds in the single-step concerted pathway. Here the thermal [1,3] sigmatropic rearrangement (see Scheme 1) of 7-*exo*-methylbicyclo[2.2.1]hept-2-ene (**2A**) to 7-*exo*-methylbicyclo [4.1.0]hept-2-ene (**2B**) has also been studied for testing the above assumption. The extensive search on the possible pathways of **R2** locates only one probable process shown in Fig. 5 (2), in which only one transition state could be found along the reaction path. Just like the

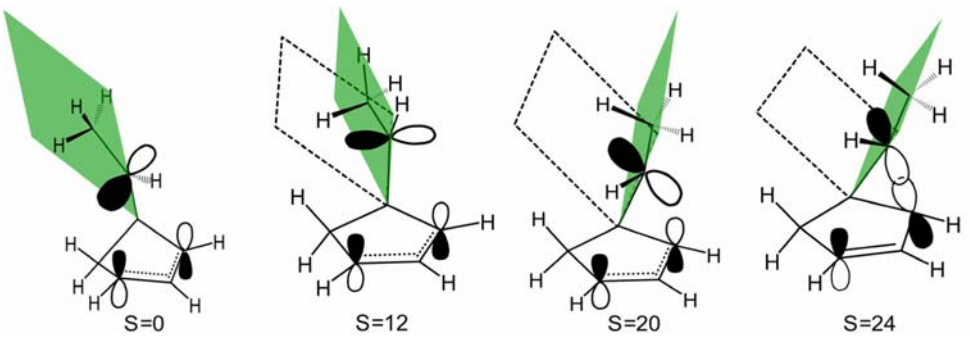

Fig. 2 The inversion of C5 and orbital overlap between C5 and C3 along reaction path

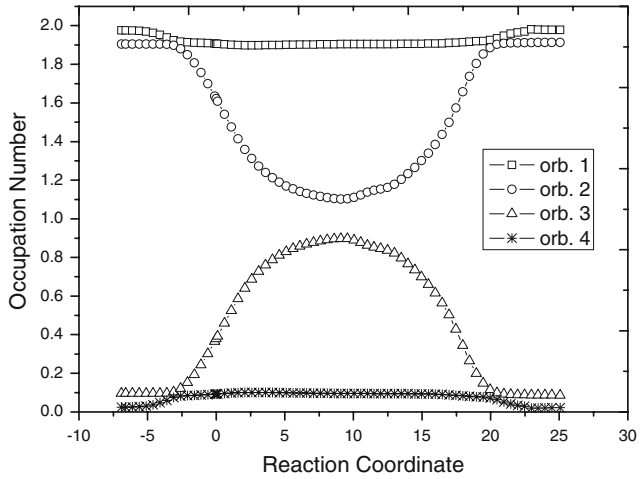

Fig. 3 Changes of populations of four active orbitals of stationary points in **R1**

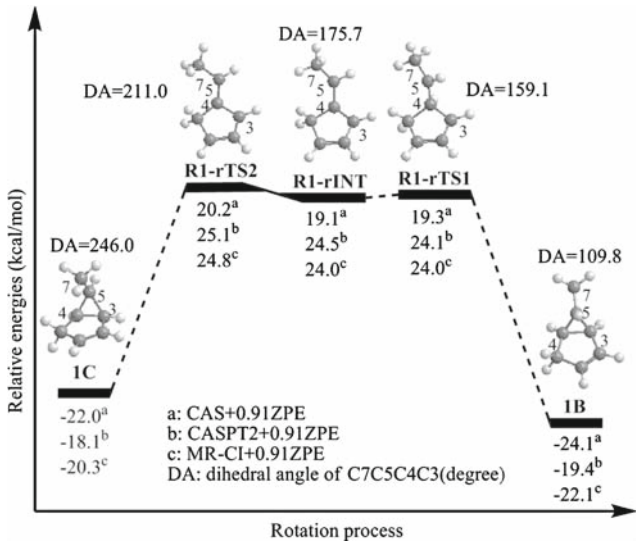

Fig. 4 Potential energy profiles for the rotation along C4–C5 in **R1**

situation of **R1**, there is also a broad region that behaves like typical diradical character, in which no true minimum can be located.

The energy barrier for this reaction is about double as that in **1A** → **1B**, reaching about 52 kcal/mol with CAS calculations. However, the reverse process has 49 kcal/mol of the energy barrier with the same calculation method. Such big difference for the energy barrier comes probably from the stability of **2A** with less ring strain compared to **1A**. The stability of **2A** over **2B** was predicted to be 8.3(CASPT2) or 8.7 kcal/mol (G2 calculation). Up to now, no thermal rearrangement process has been reported in the literatures, which is waiting for the confirmation from experiments. The suggested experimental temperature should be above 250 °C for the [1,3] sigmatropic rearrangement of **2B** to **2A**.

R3 and **R4**. For these type reactions, there are mainly three types of movements along the reaction paths. After C1–C7 bond is broken, there are two torsional movements, i.e., along C5–C6 and C7–C6. Therefore, the reaction mechanisms become more complicated and the [1,3] sigmatropic rearrangements of **3A** and **4A** show more visible stepwise characters. Along the flat regions of the potential energy profiles for reactions **R3** and **R4**, some corresponding diradical intermediate species are located, respectively (see Figs. 6, 7), and then suprafacial inversion (SI) and suprafacial retention (SR) pathways are located, respectively, which correspond to the two probable torsional movements when the C–C bond is broken. From the known literatures, one can realize that both the SI products and SR products are observed, and the SI product is still preponderant over SR product.

Computed results demonstrated that the [1,3] sigmatropic rearrangement of **3A** can yield two different products via two different pathways: (a) **3A** → **R3-INT1** → **3B**; (b) **3A** → **R3-INT1** → **R3-INT2** → **3C**, in which the pathway (a) leads to the SI product **3B**, and the pathway (b) produces the SR product **3C**. The values of bond lengths of C7–C1 and C7–C3 and the dihedral angles of C7C6C5C4 and C8C7C6C5 are shown in Scheme 3. The reaction starts with the breaking of C1–C7 bonding to form an intermediate **R3-INT1**, which is a typical diradical intermediate as the populations of four active orbitals are 1.90, 1.10, 0.89, and 0.10, respectively. Comparison of the evolvement of the dihedral angle C7C6C5C4 from **3A** to **R3-INT1** indicates that the rotation

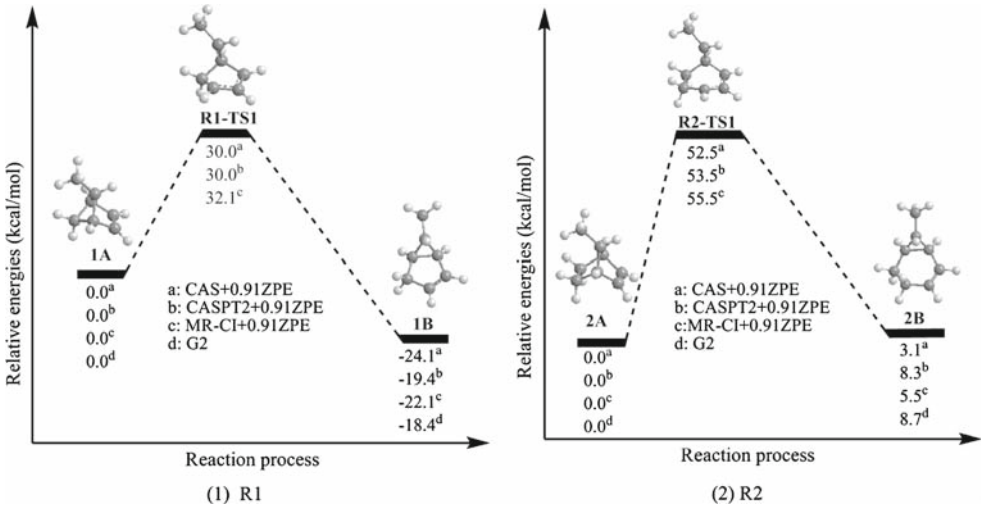

Fig. 5 Potential energy profiles for reactions **R1** and **R2**

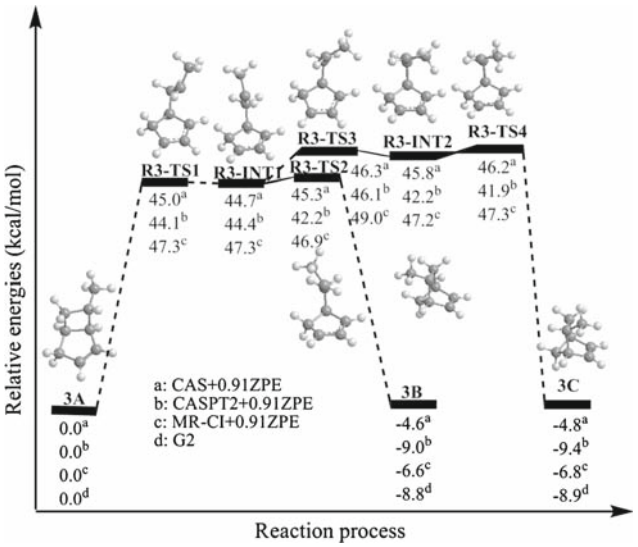

Fig. 6 Potential energy profile for reaction **R3**

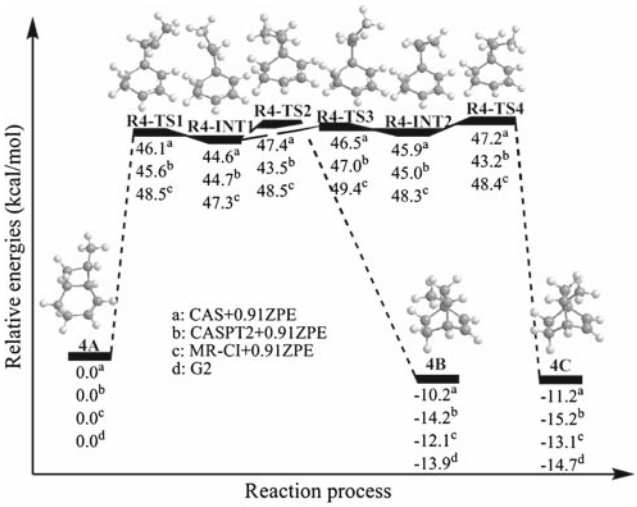

Fig. 7 Potential energy profile for reaction **R4**

movement around C6–C5 is tempered as the C7–C1 is broken. The breaking of C1–C7 needs to climb a transition state **R3-TS1**, in which the distance of C1-C7 is 2.741 Å that is between 1.551 Å in **3A** and 3.085 Å in **R3-INT1**. After **R3-INT1**, the reaction can proceed in two different ways: one is the direct cyclization to form SI product **3B**, and another is involved in a rotation movement along the C6–C7 bond and the formation of C3–C7 bond, in which a diradical intermediate **R3-INT2** is located before the formation of product **3C**.

The CAS(4,4)/6-31G(d,p) relative energies with zero-point energy corrections are depicted in Fig. 6, along with CASPT2 and MR-CI single-point relative energies with CASSCF zero-point energy corrections, which is similar to that of the [1,3] shift of bicycle[3.2.0]hept-2-ene previously explored by Houk group [40,41]. From Fig. 6, one can observe that the MR-CI calculation elevates the relative energies for most transition states and intermediates by about 2–3 kcal/mol energy, but it lowers about 2 kcal/mol relative energies for the final products, and CASPT2 calculations shift a little down the relative energies of transition states, intermediates as well as products. It should be noted that the energy of **R3-INT1** is little lower than those of **R3-TS1** and **R3-TS2** with CASSCF calculation, but higher with CASPT2 calculation, and almost same with MR-CI calculation, which indicate that such intermediates are not in a deep well. Comparison of the relative energy of **R3-TS2** with that of **R3-TS3** reveals that SI process is slightly easier than SR one as the energy difference between these two transition states reaches 1.0, 3.9 and 2.1 kcal/mol with CASSCF, CASPT2

Scheme 3 [1,3] Sigmatropic rearrangement of **3A** (all distances are in Å and all angles are in degree)

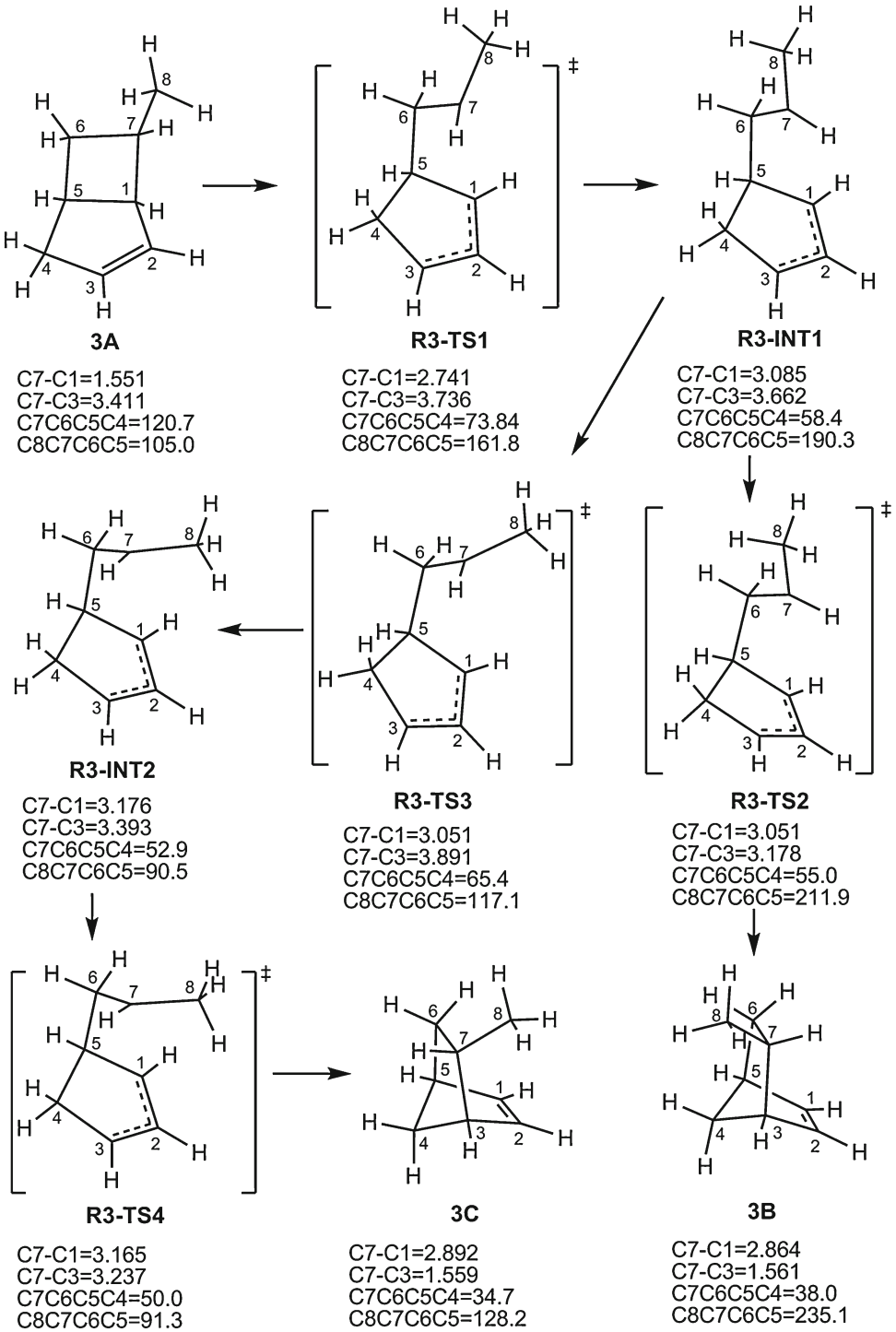

and MR-CI calculations, respectively, indicating that the more electron correlation favors the stability of **R3-TS2**. Moreover, the intermediate **R3-INT1** is very unstable, which could quickly turn into more stable **3B** or go back to **3A**, or form another unstable intermediate **R3-INT2** and then to final product **3C**. It can be assumed that the possibility of the first case should be larger both thermodynamically and kinetically, and the yield of **3C** will also be foreclosed by the multiple steps, in which **R3-INT1** is rearranged to another close stability of intermediate **R3-INT2** and then this intermediate undergoes the formation of a new C–C bond to form the final SR product of **3C**. The relative energies for the intermediates and transition states are within 50 kcal/mol, about 20 kcal/mol higher than that of the rearrangement of

Scheme 4 [1,3] Sigmatropic rearrangement of **4A** (all distances are in Å and all angles are in degree)

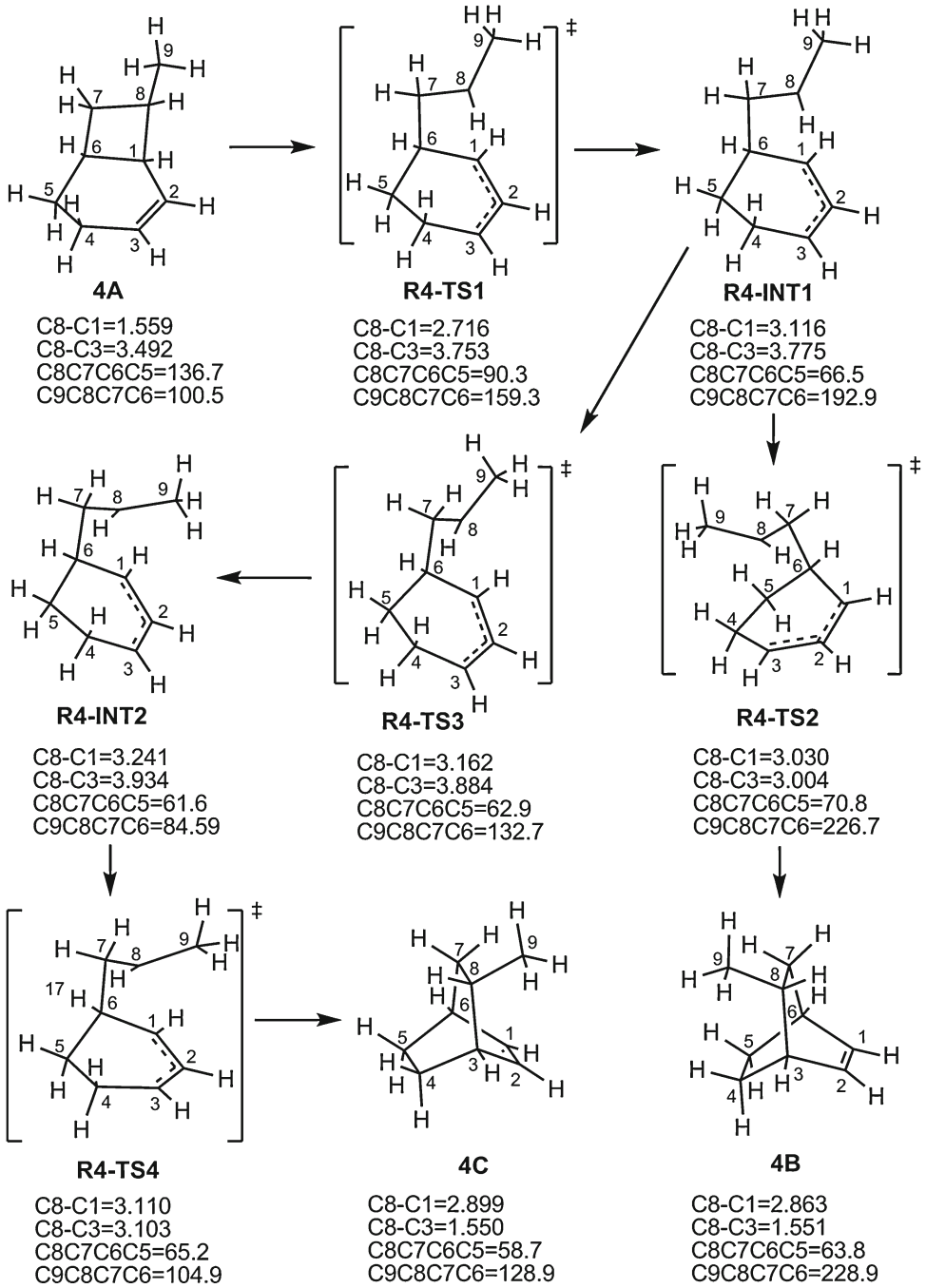

1A. These results are in consistence with those experimental conditions that **1A** could proceed [1,3]-sigmatropic rearrangement at 120 °C, while the reaction of **3A** could undergo at the range of 250–300 °C.

According to Carpenter's dynamic-controlling theory [42], the preponderant SI outcome **3B** is from the advantaged rotation around C6–C7 bond. The plateaus on the PES of **R3** offer a good stage to verify this perspective. Extensive attempts to locate the single-step concerted transition state that connects directly **3A** with **3B** is not successful at CASSCF calculation. Comparing the flat regions on the PES of **R3** with that of **R1**, the diradical stationary points that were characterized with true minima could be located along the plateaus of **R3**.

The [1,3] sigmatropic rearrangement of **4A** is very similar to that of **3A** in mechanism (see Scheme 4), in which both SI pathway to **4B** and SR pathway to **4C** start at the same diradical intermediate **R4-INT1** that originates from **4A** via a transition state **R4-TS1**. The intermediate **R4-INT1** is still a diradical, since the calculated populations of four

Scheme 5 [1,3] Sigmatropic rearrangement of **5A** (all distances are in Å and all angles are in degree)

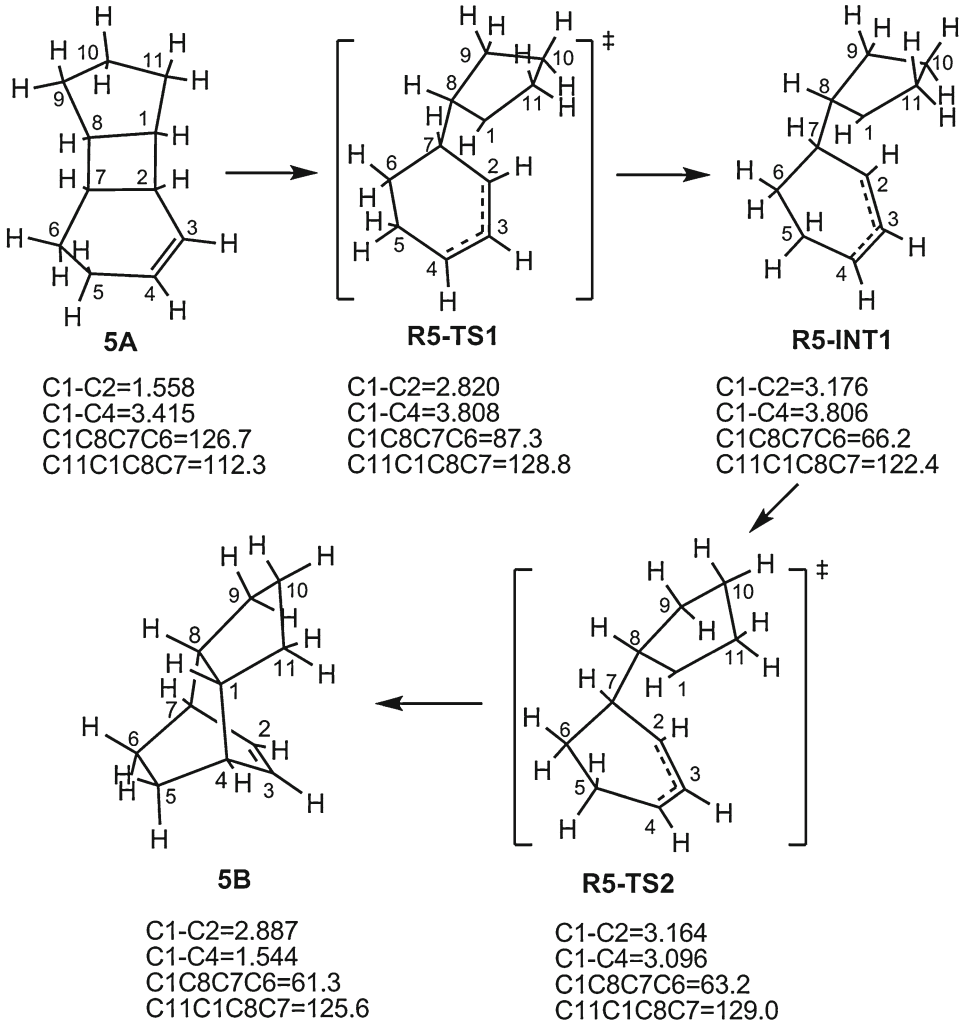

active orbitals of **R4-INT1** are 1.90, 1.00, 0.95, and 0.10, respectively.

Potential energy profile for this reaction in Fig. 7 is very similar to that in Fig. 6, except that the relative energies for two key transition states **R4-TS2** and **R4-TS3** are calculated to be closer, which are 3.5 and 0.9 kcal/mol with CASPT2 and MR-CI calculations, respectively. This is the reason why the ratio of SI/SR is decreased from about 6.8 (for **R3**) to 2.4 (for **R4**). However, as stated previously, the yield of **4C** might be decreased as the intermediate **R4-INT2** could proceed to **4C** and back to **R4-INT1** with almost the same barrier, which leads to that the yield for SI obtained is always over that of SR despite of different values for different cases.

From Carpenter's perspective [42], the increasing flexility of system reduces the superiority of SI product, and so the ratio of SI/SR decreases. Extensive search on this potential energy surface, the so-called concerted transition state that connects directly **4A**with **4B** cannot be found at CASSCF level.

R5. The [1,3] rearrangement reaction of **5A** proceeds via the only SR pathway (Scheme 5), as the cyclopentane structure restricts the rotation about C1–C8 bond in **R5-INT1** when C1–C2 bonding is broken. From **5A** to **R5-INT1**, two main reaction coordinates dominate the process, one of which is the bond length of C1–C2 and another is the torsional angle of C1C8C7C6. The evolvement of C1–C2 bond length is dramatically fast before **R5-TS1** and it reaches the maximum 3.18 Å in **R5-INT1**, while the change of C1–C4 is mainly after **R5-TS2**. At the same time, the rotation movement around C8–C7 is also ceased at **R5-INT1**. As more repulsion strain exists for the present system, the calculated bond lengths of C1–C2 and C1–C4 are a little longer than those corresponding values in other systems. From the potential energy profile in Fig. 8, one can observe that the activation barrier is about 2–3 kcal/mol higher than that of **3A** → **3B** (or **3C**) or **4A** → **4B** (or **4C**), which is expected from the fact that the reaction temperature is the highest one among those studied reactions. Also, the relative energy of product **5B** with CASPT2 calculation is closest to the G2 energy. Like other reactions discussed above, the plateau also exists in the PES of **R5**, but the so-called one-step process does not exist from our extensive search.

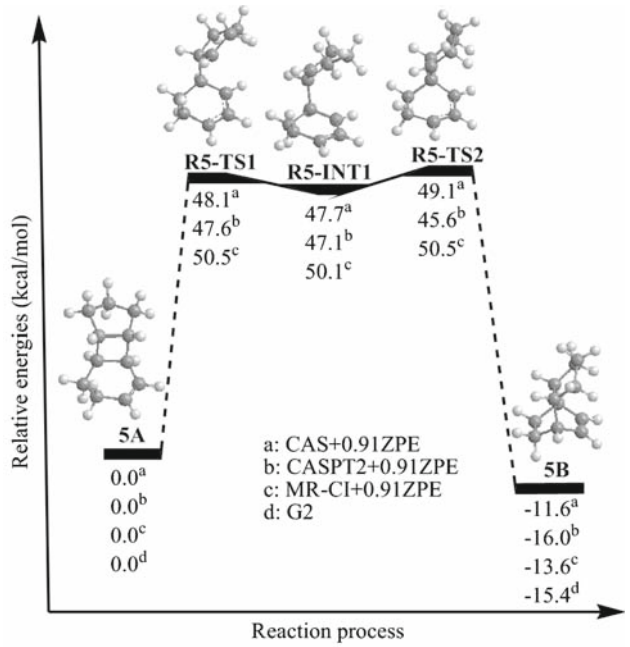

Fig. 8 Potential energy profile for reaction **R5**

4 Conclusions

Not the traditional concerted or stepwise mechanism, but a gray zone between these two extremes is appropriate to describe the mechanism of [1,3] sigmatropic rearrangement of vinylcyclobutanes. Characteristic flat regions on the PESs provide a basis for our conclusions.

For the reactions **1A** and **2A,**the reaction proceeds in more-like one-step process, the reason for this is that only one C–C rotation movement exists when the bridged C–C is opened.

For the reactions **3A** and **4A**, the stepwise mechanisms seem more obvious because there exist two C–C rotation movements when the bridged C–C is broken.

For reaction **5A**, only one type of product could be formed due to geometric restraint and the reaction proceeds in stepwise one.

Acknowledgments De-Cai Fang thanks the National Nature Science Foundation of China (20773016), the program for New Century Excellent Talents in University (NCET-04-0146), the Major State Basic Research Development Programs (2004CB719900) for financial support, and the High-powered computing center of Beijing Normal University for partial CPU times.

References

1. Woodward RB, Hoffmann R (1965) J Am Chem Soc 87:2512
2. Hoffmann R, Woodward RB (1965) J Am Chem Soc 87:4389
3. Woodward RB, Hoffmann R (1969) Angew Chem Int Ed Engl 8:781
4. Woodward RB, Hoffmann R (1970) The Conservation of Orbital Symmetry. Academic Press, New York
5. Berson JA, Nelson GL (1967) J Am Chem Soc 89:5503
6. Berson JA, Nelson GL (1970) J Am Chem Soc 92:1096
7. Berson JA (1972) Acc Chem Res 5:406
8. Frey HM (1966) Adv Phys Org Chem 4:148
9. Frey HM, Walsh R (1969) Chem Rev 69:103
10. Roth WR, Friedrich A (1969) Tetrahedron Lett 31:2607
11. Baldwin JE, Belfield KD (1988) J Am Chem Soc 110:296
12. Klärner FG, Drewes R, Hasselmann D (1988) J Am Chem Soc 110:297
13. Bender JD, Leber PA, Lirio RR, Smith RS (2000) J Org Chem 65:5396
14. Bogle XS, Leber PA, Mccullough LA, Powers DC (2005) J Org Chem 70:8913
15. Benson JA, Holder RW (1973) J Am Chem Soc 95:2037
16. Baldwin JE, Bogdan AR, Leber PA, Powers DC (2005) Org Lett 7:5195
17. Frisch MJ, Trucks GW, Schlegel HB, Scuseria GE, Robb MA, Cheeseman JR, Montgomery JA, Vreven T Jr, Kudin KN, Burant JC, Millam JM, Iyengar SS, Tomasi J, Barone V, Mennucci B, Cossi M, Scalmani G, Rega N, Petersson GA, Nakatsuji H, Hada M, Ehara M, Toyota K, Fukuda R, Hasegawa J, Ishida M, Nakajima T, Honda Y, Kitao O, Nakai H, Klene M, Li X, Knox JE, Hratchian HP, Cross JB, Adamo C, Jaramillo J, Gomperts R, Stratmann RE, Yazyev O, Austin AJ, Cammi R, Pomelli C, Ochterski JW, Ayala PY, Morokuma K, Voth GA, Salvador P, Dannenberg JJ, Zakrzewski VG, Dapprich S, Daniels AD, Strain MC, Farkas O, Malick DK, Rabuck AD, Raghavachari K, Foresman JB, Ortiz JV, Cui Q, Baboul AG, Clifford S, Cioslowski J, Stefanov BB, Liu G, Liashenko A, Piskorz P, Komaromi I, Martin RL, Fox DJ, Keith T, Al-Laham MA, Peng CY, Nanayakkara A, Challacombe M, Gill PMW, Johnson B, Chen W, Wong MW, Gonzalez C, Pople JA, Gaussian, Inc., Wallingford CT (2004) Gaussian 03, revision C.02
18. Schmidt MW, Baldridge KK, Boatz JA, Elbert ST, Gordon MS, Jensen JJ, Koseki S, Matsunaga N, Nguyen KA, Su S, Windus TL, Dupuis M, Montgomery JA (1993) J Comput Chem 14:1347
19. Ishida K, Morokuma K, Komornicki A (1977) J Chem Phys 66:2153
20. Muller K (1980) Angew Chem Int Ed Engl 19:1
21. Schmidt MW, Gordon MS, Dupuis M (1985) J Am Chem Soc 107:2585
22. Garrett BC, Redmon MJ, Steckler R, Truhlar DG, Baldridge KK, Bartol D, Schmidt MW, Gordon MS (1988) J Phys Chem 92:1476
23. Baldridge KK, Gordon MS, Steckler R, Truhlar DG (1989) J Phys Chem 93:5107
24. Gonzales C, Schlegel HB (1989) J Chem Phys 90:2154
25. Stewart JJP, Davis LP, Burggraf LW (1987) J Comput Chem 8:1117
26. Maluendes SA, Dupuis M (1990) J Chem Phys 93:5902
27. Taketsugu T, Gordon MS (1995) J Phys Chem 99:8462
28. Gordon MS, Chaban G, Taketsugu T (1996) J Phys Chem 100:11512
29. Takata T, Taketsugu T, Hirao K, Gordon MS (1998) J Chem Phys 109:4281
30. Sadtler Standard Grating Spectra (1975) Sadtler Research Laboratories, Inc., Subsidiary of Block Engineering, Inc 35584K
31. Werner HJ, Knowles PJ (1988) J Chem Phys 89:5803
32. Knowles PJ, Werner HJ (1988) Chem Phys Lett 145:514
33. Hrovat DA, Morokuma K, Borden WT (1994) J Am Chem Soc 116:1072
34. Hrovat DA, Borden WT (2001) J Am Chem Soc 123:4069
35. Werner HJ (1996) Mol Phys 89:645
36. Suhdrada CP, Houk KN (2002) J Am Chem Soc 124:8796

37. Newman-Evans RH, Simon RJ, Carpenter BK (1990) J Org Chem 55:695
38. Carpenter BK (1992) J Org Chem 57:4645
39. Leigh WJ, Srinivasan R (1983) J Org Chem 48:3970
40. Beno BR, Wilsey S, Houk KN (1999) J Am Chem Soc 121:4816
41. Wilsey S, Houk KN, Zewail AH (1999) J Am Chem Soc 121:5772
42. Carpenter BK (1995) J Am Chem Soc 117:6336